

# **Polymersomes: Tough Vesicles Made from Diblock Copolymers**

**Bohdana M. Discher, You-Yeon Won, David S. Ege, James C-M. Lee,  
Frank S. Bates, Dennis E. Discher,\* and Daniel A. Hammer\***

Vesicles were made from amphiphilic diblock copolymers and characterized by micromanipulation. The average molecular weight of the specific polymer studied, polyethyleneoxide-polyethylethylene (EO<sub>40</sub>-EE<sub>37</sub>), is several-fold greater than that of typical phospholipids in natural membranes. Both the membrane bending and area expansion moduli of electroformed polymersomes (polymer-based liposomes) fell within the range of lipid membrane measurements, but the giant polymersomes proved to be almost an order of magnitude tougher and sustained far greater areal strain before rupture. The polymersome membrane was also at least tenfold less permeable to water than common phospholipid bilayers. The results suggest a new class of synthetic thin-shelled capsules based on block copolymer chemistry.

---

B.M. Discher, D.S. Ege, J.C.M. Lee, D.E. Discher, and D.A. Hammer, School of Engineering and Applied Science, and Institute for Medicine and Engineering, University of Pennsylvania, Philadelphia, PA 19104-6315, USA. Y.-Y. Won and F.S. Bates, Department of Chemical Engineering and Materials Science, University of Minnesota, Minneapolis, MN 55455, USA.

\* To whom correspondence should be addressed at School of Engineering and Applied Science, University of Pennsylvania, Philadelphia, PA 19104-6315, USA.

*Keywords: amphiphile, block copolymer, vesicle, liposome, encapsulation*

Amphiphilic block copolymers in water, like natural phospholipids, can self-assemble into various ordered mesophases (1-3), notably lamellar structures. The symmetry and stability of the microstructure depends intimately on chain size and chemistry as well as physical variables such as temperature  $T$ . At dilute concentrations of natural amphiphiles in water, bilayer structures with a thickness of only a few nanometers can form; for cells, such membranes have permeability, stability, and mechanical characteristics that are central to function (3, 4). These characteristics also affect how liposomes and their complexes encapsulate and deliver active agents (5). Small amphiphiles of natural origin have inspired higher molecular weight, synthetic analogs defined as superamphiphiles (6), which include linear diblock copolymers composed of a serial tandem of hydrophilic and hydrophobic chains. We report here some of the properties of membranes assembled from one such superamphiphile, polyethyleneoxide-polyethylethylene [EO<sub>40</sub>-EE<sub>37</sub>; number-average molecular weight  $M_n = 3900$  g/mol (1, 7)]. This neutral, synthetic polymer has a mean contour length ( $\approx 23$  nm) approximately 10 times that of a typical phospholipid acyl chain (Fig. 1A). Chains of PEO, also referred to as PEG, are also notable for imparting biocompatibility to membranes (8). The specific diblock copolymer studied here had previously been synthesized as one chain, designated OE-7, among a low polydispersity series with varied molecular weights and block size distributions (7); OE-7 was shown to have a robust propensity to form a lamellar phase in water over a broad range of concentrations and temperatures (25 °C included) (1).

Small, non-aggregating vesicles ( $\approx 200$  nm) assembled from OE-7 were first observed by cryogenic transmission electron microscopy (cryo-TEM) after hydration and preparative vitrification (Fig. 1B) (9). Worm-like micelles (2) as well as spherical micelles coexist with the vesicles. Imaging of the hydrophobic cores of these structures revealed a core thickness  $d = 8$  nm significantly greater than  $d = 3$  nm for phospholipid bilayers (3). To facilitate detailed characterization of the material properties of block copolymer lamellae, giant vesicles (from 20 to 50  $\mu$ m) of OE-7 were made by electroformation (10), a process in which a thin film of polymer on

adjacent electrodes was phoresed by alternating current into aqueous solution. Thermal undulations of the quasi-spherical polymersome membranes provided an immediate indication of membrane softness (Fig. 2A). Furthermore, if the vesicles were made in the presence of either a 10-kD fluorescent dextran (Fig. 2B) or a protein such as globin, the probe was found to be readily encapsulated and retained by the vesicle for at least several days. The polymersomes further proved highly deformable and could be aspirated into micrometer-diameter pipettes (Fig. 2, C and D) (10).

The elastic behavior of a polymersome membrane in micropipette aspiration (at  $\sim 23^\circ\text{C}$ ), appeared comparable in quality to a fluid phase lipid membrane. Analogous to a lipid bilayer, at low but increasing aspiration pressures, the thermally undulating polymersome membrane was progressively smoothed, increasing the projected area logarithmically with tension,  $\gamma$ , (Fig. 3A). From the slope of this increase versus the fractional change,  $\Delta A/A$ , in vesicle area the bending modulus,  $K_b$ , was calculated (11)

$$K_b = k_B T \ln(\Delta A/A) / (8 \gamma) + \text{constant}$$

and found to be  $1.4 \pm 0.3 \times 10^{-19}$  J (6 vesicles) ( $k_B$  is Boltzmann's constant). Above a crossover tension  $\gamma_x$ , a renormalized area expansion modulus (11),  $K_a$ , was obtained from the relation

$$K_a = \gamma / (\Delta A/A)$$

Aspiration in this regime primarily corresponds to a true -- rather than a projected -- reduction in molecular surface density, and, for the polymersome membranes,  $K_a = 120 \pm 20$  mN/m (21 vesicles). Fitted moduli were checked for each vesicle by verifying that the crossover tension,  $\gamma_x = (K_a / K_b) (k_B T / 8 \gamma)$ , suitably fell between appropriate high tension (membrane stretching) and low tension (membrane smoothing) regimes. Measurements of both moduli,  $K_a$  and  $K_b$ , were further found to yield essentially unimodal distributions with small enough standard deviations ( $\lesssim 20\%$  of mean) to be considered characteristic of unilamellar PEO-PEE vesicles. Interestingly, the moduli are also well within the range reported for various pure and mixed lipid membranes. SOPC (1-stearoyl-2-oleoyl phosphatidylcholine) in parallel manipulations was found, for example,

to have  $K_a = 180$  mN/m (Fig. 3B) and  $K_b = 0.8 \times 10^{-19}$  J, which are largely identical to prior measures (4, 11). Lastly, at aspiration rates where projection lengthening was limited to  $<1$   $\mu\text{m/s}$ , the microdeformation proved largely reversible, consistent again with an elastic response.

The measured  $K_a$  is most simply approximated by four times the surface tension,  $\gamma$ , of a pure hydrocarbon-water interface ( $\gamma = 20 - 50$  mJ/m<sup>2</sup>), and thus reflects the summed cost of two monolayers in a bilayer (12). The softness of  $K_a$  compared to gel or crystalline states of lipid systems is further consistent with liquid-like chain disorder (13); indeed, because the average interfacial area per chain,  $\langle A_c \rangle$ , in the lamellar state has been estimated to be  $\langle A_c \rangle \gtrsim 2.5$  nm<sup>2</sup>/molecule (1), the root-mean-squared area fluctuations at any particular height within the bilayer can also be estimated to be, on average,  $\langle A_c^2 \rangle^{1/2} = (\langle A_c \rangle k_B T / K_a)^{1/2} \gtrsim 0.3$  nm<sup>2</sup>/molecule, which is a significant fraction of  $\langle A_c \rangle$  and certainly not small on a monomer scale. Moreover, presuming in the extreme, a bilayer of unconnected monolayers  $d/2$  thick, with  $d$  estimated from cryo-TEM (Fig. 1), the PEE contour length is more than twice the monolayer core thickness and therefore configurationally mobile along its length. In addition, molecular theories (14) of chain packing in bilayers have suggested that, although at a fixed area per molecule there is a tendency for  $K_b$  to increase with chain length (that is membrane thickness) other factors such as large  $\langle A_c \rangle$  can act to reduce  $K_b$ . Thus, despite the large chain size of OE-7, a value of  $K_b$  similar to that of lipid bilayers is not unduly surprising. Related to the length scales above, the root ratio of moduli,  $(K_b/K_a)^{1/2}$ , is generally recognized (3, 4, 14, 15) as providing a proportionate measure of membrane thickness. For the OE-7 membranes studied here,  $(K_b/K_a)^{1/2} = 1.1$  nm on average. In comparison to fluid bilayer vesicles of phospholipids or phospholipids plus cholesterol, where the latter often have the highest  $K_a$ , it has been reported that  $(K_b/K_a)^{1/2} = 0.53$  to  $0.69$  nm (11). A parsimonious continuum model for relating such a length scale to structure is based on the idea that the unconnected monolayers of the bilayer have, effectively, two stress-neutral surfaces located near each hydrophilic-hydrophobic core interface (15). If we assume that a membrane tension resultant may be located both above and below each interface, then

$$(K_b/K_a) = H C$$

where  $H$  and  $C$  are, respectively, distances from the neutral surfaces into the hydrophilic and hydrophobic cores. For lipid bilayers with  $d/2 = 1.5$  nm and hydrophilic head groups 1 nm thick, estimates of  $C = 0.75$  nm and  $H = 0.5$  nm yield a root-product  $[(H C)^{1/2} = 0.61$  nm] consistent with experiment. The numerical result for PEO-PEE membranes (1.1 nm) suggests that the stress resultants are centered further from the interface, but not, perhaps surprisingly, in strict proportion to the increased thickness nor the polymer length.

Elastic behavior terminates in membrane rupture at a critical tension,  $\sigma_c$ , and areal strain,  $\epsilon_c$ . With lipids, invariably  $\epsilon_c \lesssim 0.05$ , consistent it appears with a molecular theory of membranes under stress (16). For the polymersomes, cohesive failure occurred at  $\epsilon_c = 0.19 \pm 0.02$  (Fig. 3B). Another metric is the toughness or cohesive energy density which, for such a fluid membrane, is taken as the integral of the tension with respect to areal strain, up to the point of failure:

$$E_c = \frac{1}{2} K_a \epsilon_c^2$$

For a range of natural phospholipids mixed with cholesterol, the toughness has been systematically measured, with  $E_c$  ranging from 0.05 to 0.5 mJ/m<sup>2</sup> (17). The OE-7 membranes, in comparison, are 5 to 50-fold tougher with  $E_c = 2.2$  mJ/m<sup>2</sup>. On a per molecule (18) rather than a per area basis, such critical energies are remarkably close to the thermal energy,  $k_B T$ , whereas such an energy density for lipid bilayers is a small fraction of  $k_B T$ . This difference indicates, for this relatively simple condensed matter system, the strong role that fluctuations in density must have in creating a lytic defect. Despite the comparative toughness of the polymersome membrane, a core "cavitation pressure",  $p_c$ , may be readily estimated as:

$$p_c = \sigma_c / d$$

yielding a value of  $p_c = 25$  atm, which falls in the middle of the range noted for lipid bilayers,  $p_c = 10$  to 50 atm (4). Bulk liquids such as water and light organics are commonly reported to have measured tensile strengths of such a magnitude, as may be generically estimated from a ratio of nominal interfacial tensions to molecular dimensions (i.e.  $\sim \sigma / d$ ). In membrane systems, this

analogy again suggests an important role for density fluctuations, which are manifested in a small  $K_a$  and which must become transversely correlated upon coalescing into a lytic defect.

Because the previous estimate for  $\langle A_c^2 \rangle^{1/2}$  is clearly not small compared to the cross section of  $H_2O$ , a finite permeability of OE-7 membranes to water is to be expected. Polymersome permeability was obtained by monitoring the exponential decay in vesicle swelling as a response to a step change in external medium osmolarity (19). The permeability coefficient,  $P_f$ , was  $2.5 \pm 1.2 \mu\text{m/s}$ . In contrast, membranes composed purely of phospholipids with acyl chains 18 carbon atoms typically have permeabilities in the fluid state at least an order of magnitude greater (25 to  $150 \mu\text{m/s}$ ) (4). The OE-7 polymersomes are thus significantly less permeable to water -- a distinction which may prove useful in application. However, on a per area basis, polymersome membranes and phospholipid membranes (with comparable  $K_a$ ) exhibit similar fluctuations in area. This leads us to postulate that the ratio of permeabilities largely reflects the relative probability for water diffusion across the membrane and decreases with relative core thickness as  $\exp(-d_{\text{OE7}}/d_{\text{lipid}})$   $e^{-8/3} = 0.07$ , which is a value close to the measured ratio of permeabilities for polymersomes versus lipid vesicles.

Vesicle morphology could be tuned by adjusting the osmotic pressure external to freely suspended polymersomes. Starting with an osmotically deflated tubular vesicle (Fig. 4), stepwise dilution of the external osmolarity lead to water permeation and swelling through a quasi-equilibrated sequence of pearled spheres, pears, and buds, to a final tensed state. After the initial pearling of the tubule, the growth of large spheres at the expense of small spheres -- a form of Ostwald ripening -- is evident. Such shape transformations of vesicle capsules, the simple red cell included, have generally been correlated with energetic costs or constraints imposed by vesicle area, the number of membrane molecules making up vesicle area, the volume enclosed by the vesicle, and the curvature elasticity of the membrane (20). More recent theoretical and experimental efforts on fluid lipid bilayers (21) have separated the curvature elasticity between a

local,  $K_B$ -scaled Helfrich term that includes a spontaneous curvature  $c_0$  and a more non-local, area-difference-elasticity term predicated on monolayer unconnectedness in spherical-topology vesicles. To oppose any relaxation of leaflet area difference, a lack of lipid transfer or "flip-flop" between layers must be postulated. Only with such a nonlocal term or  $c_0 = 0$ , it seems, can a vesicle maintain in apparent equilibrium the sorts of multisphere (21, 22) and budded morphologies observable in both lipid systems and in the osmotically deflated polymersomes. Because wormlike and spherical micelles are in evidence (Fig. 1B),  $c_0 = 0$  appears likely. However, heterogeneity in the morphology of polymersomes, both small (Fig. 1B) and large (Fig. 4) vesicles, also suggests an important contribution from monolayer area difference, a process-dependent feature that arises upon vesicle closure and may become locked in without flip-flop of the amphiphile (21).

Polymersomes, of the general type examined here, enable direct measurements of the material properties of lamellae and put to the test some basic ideas of membrane assembly. Compared to lipids, the increased length and conformational freedom of polymer chains not only provide a basis for enhanced toughness and reduced permeability of membranes but also suggest that the rich diversity of block copolymer chemistries (molecular weights, block fraction, block architecture) portends a plethora of novel, artificial membranes. Additional control over membrane properties may be afforded, for example, through selective cross-linking of block copolymer hydrocarbon chains as demonstrated with worm-like micelles (2). As with the rich variety of phospholipids and membrane modifiers, each synthetic membrane might find its own application in transport, rheology, or encapsulation, rationally based on a suitable selection of material properties, thermal behaviors, and permeabilities.

**References and Notes**

1. D.A. Hajduk, M.B. Kossuth, M.A. Hillmyer, and F.S. Bates, *J. Phys. Chem. B* 102, 4269 (1998); H.E. Warriner, S.H.J. Idziak, N.L. Slack, P. Davidson, C.R. Safinya, *Science* 271, 969 (1996). K. Yu and A. Eisenberg, *Macromolecules* 31, 3509 (1998).
2. Y.Y. Won, H.T. Davis, and F.S. Bates, *Science* (in press).
3. Reviewed in R. Lipowsky and E. Sackmann (eds.), *Structure and Dynamics of Membranes - From Cells to Vesicles*, V. 1 of the Handbook of Biological Physics, Elsevier Science B.V. (1995). Note (as tabulated on page 19 of this reference) that for a generic plasma membrane such as that of the red blood cell, approximately three-fourths of the phospholipids have acyl chains of lengths 16, 18, or 20 carbon atoms. Note also (as indicated on pages 229 or 658 of the same reference) that a bilayer of lipids with 16 or 18 carbon atom chains in the biologically relevant disordered liquid phase ( $L_d$ ) may be estimated to have a thickness  $d \approx 3$  nm.
4. M. Bloom, E. Evans, O.G. Mouritsen, *Q. Rev. Biophys.* 24, 293 (1991); D. Needham and D. Zhelev, in *Vesicles*, Morton Rosoff, ed., Dekker, NY, (1996), Ch. 9.
5. G. Cevc, Ch. 9 in (3); D.D. Lasic, Ch. 10 in (3); I. Koltover, T. Salditt, J.O. Radler, and C. Safinya, *Science* 281, 78 (1998). T.O. Harasym, P.R. Cullis, M.B. Bally, *Cancer Chemotherapy & Pharmacology* 40, 309 (1997).
6. J. Cornelissen, M. Fischer, N. Sommerdijk, R. Nolte, *Science* 280, 1427 (1998).
7. M.A. Hillmyer and F.S. Bates, *Macromolecules* 29, 6994 (1996); M.A. Hillmyer et al, *Science* 271: 976 (1996). For EO<sub>40</sub>-EE<sub>37</sub>, a polydispersity measure is given by  $M_w/M_n \sim 1.10$ , where  $M_w$  and  $M_n$  are the weight-average and number-average molecular weights, respectively. The PEO volume fraction is  $f_{EO} = 0.39$ .
8. J.M. Harris, editor, S. Zalipsky, editor, *Poly(ethylene glycol): chemistry and biological applications*, American Chemical Society, (1997). Also, as reviewed in D.D. Lasic, Ch. 10 in (3), PEG chain lengths which optimize the stealth of liposomes, i.e. lipid-conjugated PEG leading to the longest blood circulation time of liposomes, are in the approximate range of EO<sub>34</sub> to EO<sub>114</sub>.

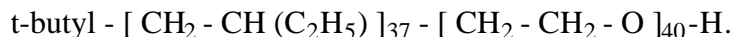
9. Thin (ca. 10 - 300 nm) films of aqueous solution suspended in a micro-perforated grid were prepared in an isolated chamber with temperature and humidity control. The sample assembly was rapidly vitrified with liquid ethane at its melting temperature (~ 90K), and this was kept under liquid nitrogen until it was loaded onto a cryogenic sample holder (Gatan 626). Images were obtained with a JEOL 1210 at 120 kV employing a nominal underfocus of 6  $\mu\text{m}$  and digital recording. For more detailed description or related examples: Z. Lin, M. He, L. E. Scriven, H. T. Davis, *J. Phys. Chem.* 97, 3571 (1993). A. Walter, P. K. Vinson, A. Kaplun, Y. Talmon, *Biophys. J.* 60, 1315 (1991).
10. EO<sub>40</sub>-EE<sub>37</sub>, synthesized by a combination of anionic polymerization and catalytic hydrogenation, was subsequently lyophilized into a solid and solubilized, when needed, in chloroform at 4 mg/ml. Evaporation of the solvent under nitrogen followed by vacuum drying for 3 to 48 h was used to deposit a film on 1 mm diameter platinum wire electrodes held in a Teflon frame (5mm separation). The Teflon frame and electrodes were assembled into a chamber by sealing with coverslips, and this was subsequently filled with 100 mM sucrose solution. To begin generating vesicles from the film, an alternating electric field was applied to the electrodes (10 Hz, 10 V) while the chamber was mounted and viewed on the stage of an inverted microscope. Giant vesicles attached to the film-coated electrode were visible after 15 - 60 min. These were dissociated from the electrodes by lowering the frequency to 3 - 5 Hz for at least 15 min. The electroformation method is adapted from that of M.I. Angelova, S. Soleau, P. Meleard, J.F. Faucon, P. Bothorel, *Prog. Coll. Polm. Sci.* 89, 127 (1992), as previously used in M.L. Longo, A.J. Waring, and D.A. Hammer, *Biophys. J.* 73, 1430 (1997). The vesicles were stable for at least several days when kept sealed from air in a gas-tight, plastic syringe. Of additional note, vesicles were stable when resuspended in physiological saline at temperatures ranging from 10 °C to 50 °C. Micromanipulation was done with micropipette systems analogous to those described in M.L. Longo et al and D.E. Discher, N. Mohandas, and E.A. Evans, *Science* 266, 1032 (1994).

11. E. Evans and W. Rawicz, *Phys. Rev. Lett.*, 64, 2094 (1990); W. Helfrich and R.-M. Servuss, *Nuovo Cimento D3*, 137 (1984); note that  $K_a$  did not differ by more than 10 to 20% from its non-renormalized value.
12. J. Israelachvili, *Intermolecular and Surface Forces*, Academic Press, NY, ed. 2, (1991).
13. E. Evans and D. Needham, *J. Phys. Chem.* 91, 4219 (1987).
14. I. Szleifer, D. Kramer, A. Ben-Shaul, D. Roux, W.M. Gelbart, *Phys. Rev. Lett.* 60, 1966 (1988); A. Ben-Shaul, Ch. 7 in (3).
15. A.G. Petrov and J. Bivas, *Progress Surf. Sci.* 18, 359 (1984).
16. R.R. Netz and M. Schick, *Phys. Rev. E* 53, 3875 (1996). Interestingly, in this and related references, the self-consistent calculation models lipids as nearly symmetric diblock copolymers which are clearly closer in form to the molecules of this study.
17. D. Needham and R.S. Nunn, *Biophys. J.* 58, 997 (1990).
18. Because the average interfacial area per chain,  $\langle A_c \rangle$ , in the lamellar state has been estimated to be  $\langle A_c \rangle \gtrsim 2.5 \text{ nm}^2/\text{molecule}$ , one estimates that  $E_c * \langle A_c \rangle \gtrsim 1.3 k_B T$ .
19. Vesicles were prepared in 100 mOsm sucrose solution which established an initial, internal osmolarity. They were then suspended in an open-edge chamber formed between coverslips and containing 100 mOsm glucose. A single vesicle was aspirated with a suction pressure sufficient to smooth membrane fluctuations; the pressure was then lowered to a small holding pressure. Using a second, transfer pipette, the vesicle was moved to a second chamber with 120 mOsm glucose. Water flows out of the vesicle due to the osmotic gradient between inside and outside, which leads to an increased projection length which is monitored over time. The exponential decrease in vesicle volume was calculated from video images and then fit to determine the permeability coefficient ( $P_f$ ) (4). For reference,  $P_f = 23.5 \pm 1.7 \text{ } \mu\text{m/s}$  for SOPC from this method.
20. H.J. Deuling and W. Helfrich, *J. Phys.* 37, 1335 (1976); S. Svetina and B. Zeks, *Eur. Biophys.* 17, 101 (1989); U. Seifert, K. Berndl, and R. Lipowsky, *Phys. Rev. A* 44, 1182 (1991).

21. U. Seifert and R. Lipowsky, Ch. 8 in (3); H.-G. Dobreiner, E. Evans, M. Kraus, U. Seifert, M. Wortis, *Phys. Rev. E* 55, 4458 (1997).
22. S. Chaieb and S. Rica, *Phys. Rev. E* 58, 7733 (1998).
23. We thank E.A. Evans, D. Needham, P. Nelson, and T. Lubensky for discussions. Support was primarily provided by the NSF-supported Materials Research Science and Engineering Center (MRSEC) at the University of Pennsylvania (DMR96-32598) and both the Center for Interfacial Engineering (CIE) and the MRSEC at the University of Minnesota. The work was also supported in part by grants from the Whitaker Foundation (DD) and NIH R01-HL62352-01(DD).

## Figures

**Fig. 1.** Molecular assemblies and copolymer structures in water. (A) Schematic representation of diblock copolymer EO<sub>40</sub>-EE<sub>37</sub>, also designated OE-7, with chain structure



The number-average molecular weight is approximately 3900 g/mol. For a simple comparison of relative hydrophobic core thickness  $d$ , a bilayer of typical lipids (3) are schematically shown next to the assembly of copolymers. (B) Aqueous suspensions of OE-7 vesicles in dominant coexistence with rod-like (black arrow) and spherical (gray arrow) micelles. Observations were made by cryo-TEM (9); the scale bar at lower left is 20 nm, and the mean lamellar thickness is  $\sim 8$  nm.

**Fig. 2.** Giant unilamellar vesicles of EO<sub>40</sub>-EE<sub>37</sub>. (A) Vesicle immediately following electroformation; the membrane is seen to be thermally undulating. (B) Encapsulation of a 10 kDa Texas Red-labeled dextran. (C and D) Microdeformation of a polymersome. The arrow marks the tip of an aspirated projection as it is pulled by negative pressure,  $P$ , into the micropipette. Aspiration acts to: (i) increase membrane tension,  $\sigma = \frac{1}{2} P R_p / (1 - R_p / R_s)$ , where  $R_p$  and  $R_s$  are the respective radii of the micropipette and the outer spherical contour; and (ii) expand the original, projected vesicle surface area,  $A_0$ , by the increment  $\Delta A$  or area fraction  $\Delta A / A_0$ .

**Fig. 3.** Mechanical properties of polymersome membranes as assessed by micromanipulation.

(A) Membrane elasticity revealed in membrane tension versus areal expansion. Filled circles indicate aspiration; open circles indicate graded release. The upper left inset shows the distribution of measurements for the bending modulus,  $K_b$ , as obtained from the initial phase of aspiration. The lower right inset shows the distribution of measurements for the area expansion modulus,  $K_a$ , as obtained from the linear phase of aspiration. (B) Membrane toughness determined by aspiration to the point of rupture (\*). For comparison, aspiration to the point of rupture of an electroformed SOPC lipid vesicle is also shown.

**Fig. 4.** Shape transformations driven by osmotic swelling of a single polymersome and imaged in phase contrast video microscopy. The vesicle was formed in 100 mOsm sucrose and the external sucrose solution was progressively diluted with distilled water from approximately 150 mOsm glucose over a period of 90 min. State A is a giant tubular state which swells with the initial appearance (state B) of interconnected spheres (inset) that conserve vesicle topology. This is followed by coalescence and disappearance (states C to E) of the spheres prior to final transformation to a single, tensed sphere (state F).

Fig. 1

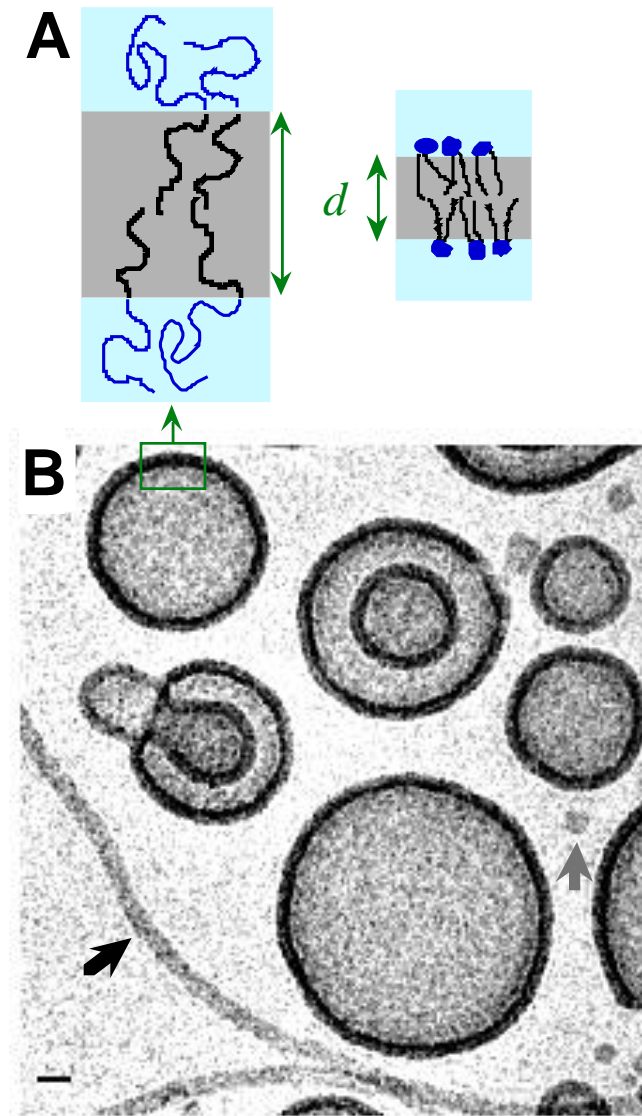


**Fig. 2**

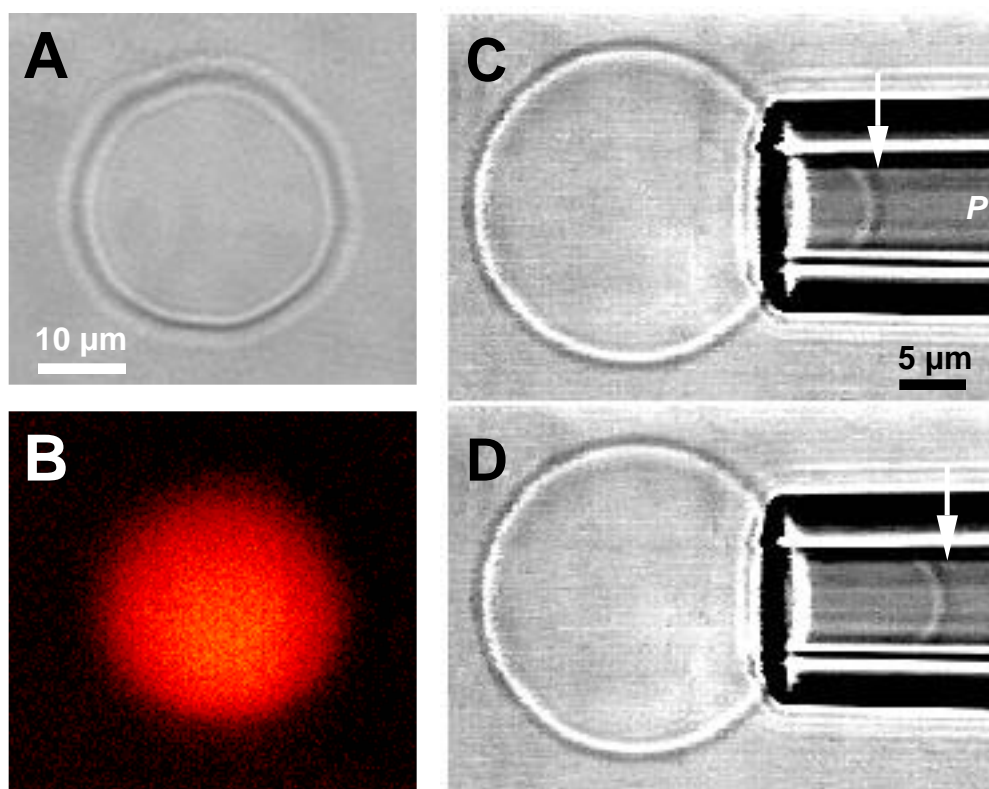


**Fig. 3**

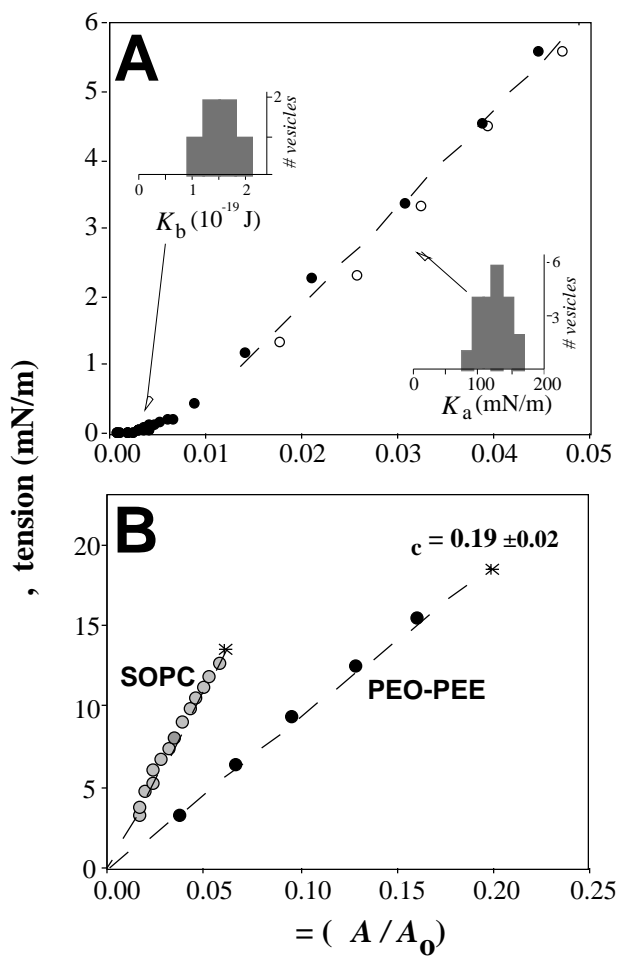


**Fig. 4**

